

qlty: handling large tensors in scientific imaging

Petrus H. Zwart^{a,b,c}

^a*Center for Advanced Mathematics in Energy Research Applications, Lawrence Berkeley National Laboratory,*

^b*Berkeley Synchrotron Infrared Structural Biology program, Lawrence Berkeley National Laboratory,*

^c*Molecular Biophysics and Integrated Bioimaging Division, Lawrence Berkeley National Laboratory, 1 Cyclotron Road, Berkeley, 94720, California, USA*

Abstract

In scientific imaging, deep learning has become a pivotal tool for image analytics. However, handling large volumetric datasets, which often exceed the memory capacity of standard GPUs, require special attention when subjected to deep learning efforts. This paper introduces `qlty`, a toolkit designed to address these challenges through tensor management techniques. `qlty` offers robust methods for subsampling, cleaning, and stitching of large-scale spatial data, enabling effective training and inference even in resource-limited environments.

Keywords: machine learning, deep learning, segmentation, denoising

1. Introduction

In computer vision applications within the experimental sciences, such as in the analysis of X-ray or Electron Tomography, Focused Ion Beam Scanning Electron Microscopy (FIB-SEM) or Adaptive Optics Lattice Light Sheet Microscopy (AO-LLSM) [1, 2, 3, 4] the use of deep learning networks for image processing and vision-related tasks has become increasingly important.

These workflows often require substantial computational resources, as data set sizes easily contain over 10^9 voxels. A significant challenge arises when training these networks, particularly with volumetric data, as the associated memory requirements for machine learning approaches on such datasets rapidly outrun the available capacity conventional hardware has to offer. For inference tasks, these issues arise as well, pushing the need for efficient data handling and processing techniques.

While distributed computing approaches, where data is shared across multiple GPUs, offer a potential solution, they are not always feasible. In scenarios involving consumer hardware or edge computing, where available resources may be significantly constrained compared to dedicated compute clusters, the problems are even more pressing. Moreover, in many scientific applications, particularly in segmentation tasks, the available labeled data can be sparse within large volumetric datasets. This sparsity presents an additional opportunity: regions of the data that lack annotations and lie outside the effective receptive field of the neural network contribute little to model training. Processing these unlabeled regions wastes valuable computational resources without improving model performance. Consequently, there is a pressing need for efficient tensor management techniques that can handle spatial data effectively in a resource-limited environment while also intelligently focusing computation on the most informative regions of sparsely annotated datasets.

Out-of-core processing methods have emerged as a crucial approach to handling datasets that exceed available memory, offering a practical solution to the challenges posed by large volumetric data in scientific computer vi-

sion [5]. These techniques typically involve data chunking, where the dataset is divided into manageable portions that can be loaded and processed sequentially, allowing for the analysis of data that far exceeds the capacity of RAM or GPU memory. While effective in many data processing scenarios, existing out-of-core methods often lack the specific functionality required for complex computer vision tasks, particularly those involving deep learning models. A key requirement for a tool to aid in these scenarios is the ability to handle overlapping subtensors, both during the chunking process and when stitching processed results back together. This capability is crucial for maintaining spatial continuity and addressing edge effects in convolutional neural networks. The absence of a light-weight tool that could efficiently manage these tasks, while also integrating seamlessly with PyTorch’s tensor operations for computer vision applications, drove the development of new methodologies to fill this gap. Such a tool needs to be capable of handling large-scale datasets, providing robust solutions for tensor patching, manipulation, and stitching.

The `qlty` toolkit addresses these challenges through a suite of specialized functions designed for tensor management in computer vision applications. By providing robust methods for tensor patching, manipulation, and stitching, `qlty` enables researchers and developers to work effectively with large-scale spatial data, even in resource-constrained environments. In this paper, we present the functionality of `qlty` and demonstrate its effectiveness through a segmentation on experimental data, illustrating how `qlty` can enable the processing of larger datasets than would otherwise be possible on limited hardware.

2. Purpose and Functionality

`qlty` is primarily aimed at providing subsampling and out-of-core tools for segmentation, denoising and related techniques in scientific imaging. A high level overview of `qlty` within these types of workflows is depicted in Figure 1

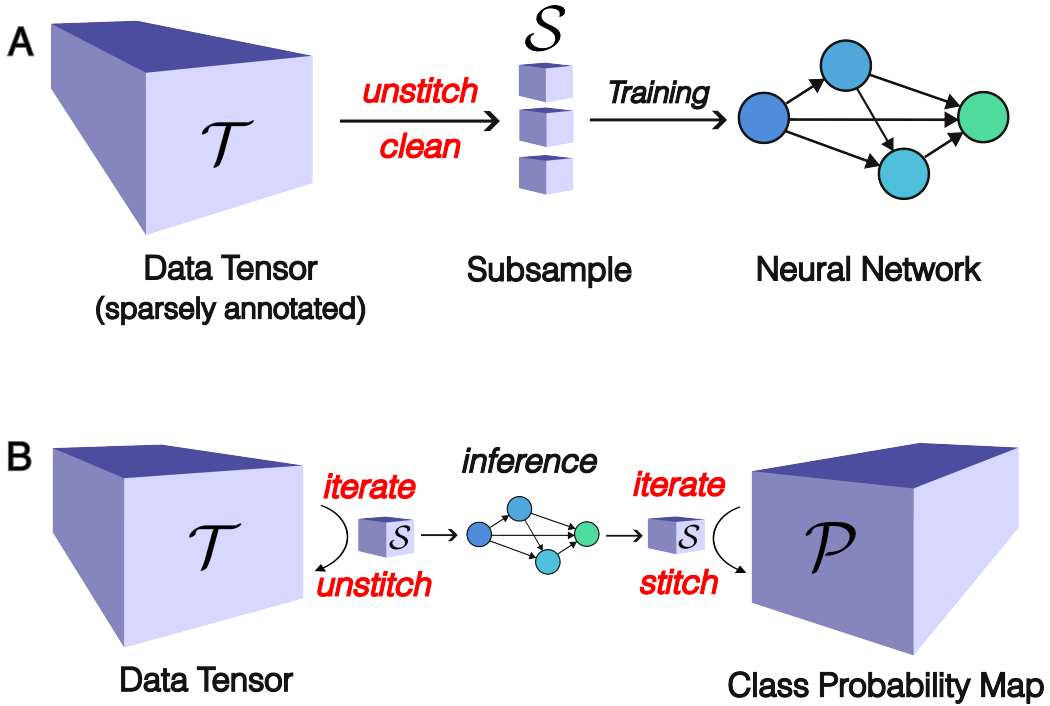


Figure 1: High level overview of `qlty` functionality. A - For generating training data with a smaller spatial footprint, `qlty` subsamples a sparsely annotated tensor \mathcal{T} into smaller chunks \mathcal{S} while discarding parts of \mathcal{T} for which no training data is available. B - In inference scenarios, `qlty` iterates over data tensor \mathcal{T} yielding manageable chunks of data that can be subjected to a neural network of choice. The resulting output is iterative placed back into a tensor of the right size.

A more detailed description of the functionality is given below.

2.1. Subsampling

Assume we have a PyTorch tensor \mathcal{T} with shape (N, C, Y, X) . This data structure contains N items of C channel data of a two-dimensional spatial map with lengths Y and X . When subsampling \mathcal{T} , the aim is to obtain tensor \mathcal{S} of size (M, C, Y_w, X_w) , where (Y_w, X_w) is referred to as the *window size*. The channel count C remains untouched, but the resulting batch size M will typically be not equal to N . Within `qlty`, the subsampling is done in a deterministic fashion by translating a window with a predefined step size across the input tensor, while deploying an step-back correction at the edges of tensor \mathcal{T} to ensure that the last subsampled window has edges aligned with the input tensor. This process is outlined for a multi-channel 2D tensors in Algorithm 1 and extends analogously to 3D scenarios.

2.2. Augmentation & Cleaning

When tensors are subsampled as described, a specific pixel or voxel from the original tensor can appear in multiple subsamples. Due to the finite size of these subsampled tensors and the receptive field of the neural network, the equivalence of identical observations across subsamples is disrupted. This issue is most evident for pixels at the edges of the subsampled tensors, which, at best, only have half the number of unique neighbors within their vicinity during convolutional calculations. When working with semantic segmentation data, a border region in the subsampled tensor can be defined, which allows us to mark data as *unobserved* and exclude these labels from the training dataset, only retaining internal voxels or pixels.

While the above procedure introduces a sparsification of the training data by excluding edge pixels or edge voxels, it is far more common that the

Algorithm 1 Subsampling Tensor \mathcal{T}

Require: \mathcal{T} of shape (N, C, Y, X) , window size (Y_w, X_w) , step size $(\text{step}_y, \text{step}_x)$

Ensure: Tensor with subsampled chunks \mathcal{S}

Initialize an empty list *subsamples*

for $n = 0$ to $N - 1$ **do**

for $y = 0$ to $Y - Y_w$ with step step_y **do**

for $x = 0$ to $X - X_w$ with step step_x **do**

$y_{\text{start}} = \min(y, Y - \text{step}_y)$

$y_{\text{stop}} = y_{\text{start}} + \text{step}_y$

$x_{\text{start}} = \min(x, X - \text{step}_x)$

$x_{\text{stop}} = x_{\text{start}} + \text{step}_x$

$\text{slice}_y = \text{slice}(y_{\text{start}}, y_{\text{stop}}, 1)$

$\text{slice}_x = \text{slice}(x_{\text{start}}, x_{\text{stop}}, 1)$

$\text{chunk} = \mathcal{T}[n : n + 1, :, \text{slice}_y, \text{slice}_x]$

 Append chunk to *subsamples*

end for

end for

end for

$\mathcal{S} = \text{concatenate}(\text{subsamples}, \text{dim} = 0)$

return \mathcal{S}

sparsity of labeled data originates from selected human labeling. In such cases, a large amount of subsampled tensors can contain no training data due to absence of labels. `qlty` provides tools to remove or exclude such tensor pairs, enriching the information content of the data, while ensuring it runs on the available hardware.

2.3. *Stitching*

Even though the memory requirements for inference are less than those for training, subsampling can still be necessary. In `qlty`, the same subsampling algorithm to generate data for inference is used as in the training scenario, without the cleaning step. In addition, accumulator arrays are created, a mean array and a normalization array, where the inference results of subsampled tensors are stored. In the mean array, inference results are multiplied by a weight term that accounts for the relative significance of predictions for border pixels and added to the accumulator. The normalization array accumulates the sum of these weights. The final prediction is obtained by calculating the weighted mean, achieved by dividing the mean array by the normalization array. Both the mean and accumulator arrays are *zarr* arrays, caching the results on disc. The final normalization is performed using *dask*, making use of multiprocessing options when available.

3. Example Usage

The use of `qlty` in a segmentation setting is illustrated by a segmentation of a 3D cryo-electron tomographic reconstruction of the cell derived matrix (CDM) produced by human telomerase immortalized foreskin fibroblasts (TIFFS) [6], publicly available via EMPIAR [7]. For illustrative purposes, a

minimal manual annotation was conducted using napari [8], where 52k pixels - the equivalent of 5 data cubes of length 64 - were labeled in a few slices across the XY,YZ and XZ projections. `qlty` was run using typical settings, with a target window of (64, 64, 64). Due to the low number of labeled pixels, a step size of 32 in all directions was used, resulting in duplicating the number of annotated pixels by a factor of 7.46, but reducing the total data volume to analyze by a factor of 9 by a subsequent elimination of subtensors without annotated data. Additional details are found in Table 3.

Training Scenario Settings	
Full Tensor shape	(1, 1, 236, 720, 510)
Annotated <i>Non Filament</i> voxels	51505
Annotated <i>Filament</i> voxels	1809
Window shape	(64, 64, 64)
Step Size	32 in Z,Y,X
Border Size	0 in Z,Y,X
Total subsample	(2310, 1, 64, 64, 64)
Clean subsample	(256, 1, 64, 64, 64)
Data duplication rate	7.47

Table 1: `qlty` training settings. Sparse labeling of a tensor, approximately 0.06% of voxels were annotated , resulted in 256 cube-like tensors of length 64. The translating window approach results in annotated data duplication - identical voxels appearing in multiple subsamples - at a rate of 7.47.

The generated training data was used to train an ensemble of eight Sparse Mixed Scale neural Networks (SMSNets) with random architecture as available from the *DLSIA* library [9]. Using Adam as an optimizer and a cross-

entropy target with a learning rate of 0.01 and batch size of 16, fifty epochs on an A100 GPU yielded an average macro F1 score - taking into account the class imbalance - of 89% and 88% for the training and validation data respectively, across all 8 models.

For inference, a larger window size is technically feasible because of lower memory requirements. Using a window size of 128, a step size of 108 and a border width of 10 were used. By setting the border weight to zero, the resulting stitching operation results in non-overlapping tensor of size (108,108,108). In this manner, 231 subtensors were generated and run through an inference pass. Further `qlty` setting are found in Table 3.

Inference Scenario Settings	
Input tensor shape	(1, 1, 236, 720, 510)
Window shape	(128, 128, 128)
Step size	108 in Z,Y,X
Border size	10 in Z,Y,X
Border weight	0 in Z,Y,X
Subsampled tensor shape	(231, 1, 128, 128, 128)
Output tensor shape	(1, 2, 236, 720, 510)

Table 2: `qlty` inference settings. Using the ensemble of trained network, inference was performed on subsampled tensors of with spatial footprint of (128,128,128), with a step size of 108 and a border size of 10. After stitching the subtensors, a tensor of shape (1,2,236,720,510) was obtained.

The results of the inference are shown in Figure 2. The high quality of the depicted segmentation originates in large part from the data augmentation by the windowed subsampling of the tensor and the associated data duplication

that follows from this procedure.

4. Impact

The `qlty` toolkit offers a light-weight solution for handling large-scale (volumetric) data for computer vision tasks in scientific imaging. By addressing the challenges associated with processing large datasets that exceed the memory capacity of typical GPUs, `qlty` enables efficient and effective image analysis in resource-constrained environments. This capability is crucial for a variety of scientific imaging applications in biology and material sciences.

`qlty` has been put to practical use in a number of applications, such as the segmentation of contaminant peaks in X-ray powder diffraction [10], the segmentation of fibers from X-ray tomography scans of reinforced concrete [9] and near-real time segmentation of X-ray tomography datasets at large scale facilities [11]. In a denoising setting, `qlty` has allowed for routine training and inference of X-ray tomographic data exceeding 10^9 pixels on a RTX-3090 NVIDIA consumer hardware gpu [12]. Training and inference on this type of data without chunking would require at least an order of magnitude more memory than the 24GB that GPU possesses, making `qlty` a indispensable tool in these workflows.

The seamless integration of `qlty` with the PyTorch framework, streamlines machine learning workflows for scientific imaging. `qlty`'s subsampling and stitching functions can be easily incorporated within existing data analytics pipelines [9], circumventing the need to write *ad-hoc* functionality that addresses these issues. `qlty` thus reduces a barrier to utilize advanced

image processing techniques in the broader scientific community.

`qlty` is available a *pip* installable package, or via <https://github.com/phzwart/qlty>.

5. Acknowledgements

We gratefully acknowledge the support of this work by the Laboratory Directed Research and Development Program of Lawrence Berkeley National Laboratory under US Department of Energy contract No. DE-AC02-05CH11231. Further support originated from the Center for Advanced Mathematics in Energy Research Applications funded via the Advanced Scientific Computing Research and the Basic Energy Sciences programs, which are supported by the Office of Science of the US Department of Energy (DOE) under contract No. DE-AC02-05CH11231, and from the National Institute of General Medical Sciences of the National Institutes of Health (NIH) under award 5R21GM129649-02. We acknowledge the use of resources of the National Energy Research Scientific Computing Center (NERSC), a U.S. Department of Energy Office of Science User Facility operated under Contract No. DE-AC02-05CH11231, under NERSC allocation m4055.

References

- [1] Mark A Le Gros, Gerry McDermott, and Carolyn A Larabell. X-ray tomography of whole cells. *Curr. Opin. Struct. Biol.*, 15(5):593–600, October 2005.
- [2] Vladan Lucić, Friedrich Förster, and Wolfgang Baumeister. Structural studies by electron tomography: from cells to molecules. *Annu. Rev. Biochem.*, 74:833–865, 2005.

- [3] C Shan Xu, Kenneth J Hayworth, Zhiyuan Lu, Patricia Grob, Ahmed M Hassan, José G García-Cerdán, Krishna K Niyogi, Eva Nogales, Richard J Weinberg, and Harald F Hess. Enhanced FIB-SEM systems for large-volume 3D imaging. *Elife*, 6, May 2017.
- [4] Güneş Parlakgöl, Ana Paula Arruda, Song Pang, Erika Cagampan, Nina Min, Ekin Güney, Grace Yankun Lee, Karen Inouye, Harald F Hess, C Shan Xu, and Gökhan S Hotamışlıgil. Regulation of liver subcellular architecture controls metabolic homeostasis. *Nature*, 603(7902):736–742, March 2022.
- [5] Alexandre Fioravante de Siqueira, Daniela M Ushizima, and Stéfan J van der Walt. A reusable neural network pipeline for unidirectional fiber segmentation. *Sci Data*, 9(1):32, February 2022.
- [6] Bettina Zens, Florian Fäßler, Jesse M Hansen, Robert Hauschild, Julia Datler, Victor-Valentin Hodiernau, Vanessa Zheden, Jonna Alanko, Michael Sixt, and Florian K M Schur. Lift-out cryo-FIBSEM and cryo-ET reveal the ultrastructural landscape of extracellular matrix. *J. Cell Biol.*, 223(6), June 2024.
- [7] Andrii Iudin, Paul K Korir, Sriram Somasundharam, Simone Weyand, Cesare Cattavittello, Neli Fonseca, Osman Salih, Gerard J Kleywegt, and Ardan Patwardhan. EMPIAR: the electron microscopy public image archive. *Nucleic Acids Res.*, 51(D1):D1503–D1511, January 2023.
- [8] napari contributors. napari: a multi-dimensional image viewer for python, 2019.

- [9] Eric J. Roberts, Tanny Chavez, Alexander Hexemer, and Petrus H. Zwart. DLSIA: Deep Learning for Scientific Image Analysis. *Journal of Applied Crystallography*, 57(2):392–402, Apr 2024.
- [10] Howard Yanxon, Eric Roberts, Hannah Parraga, James Weng, Wenqian Xu, Uta Ruett, Alexander Hexemer, Petrus Zwart, and Nickolas Schwarz. Image segmentation using u-net architecture for powder x-ray diffraction images, 2023.
- [11] Advanced Light Source News. Als computing group brings machine learning models to beamtimes around the world, July 2024. Accessed: 2024-07-05.
- [12] Odeta Qafoku, Tamas Varga, and Petrus H. Zwart. Covered affairs: denoising with confidence. In preparation.

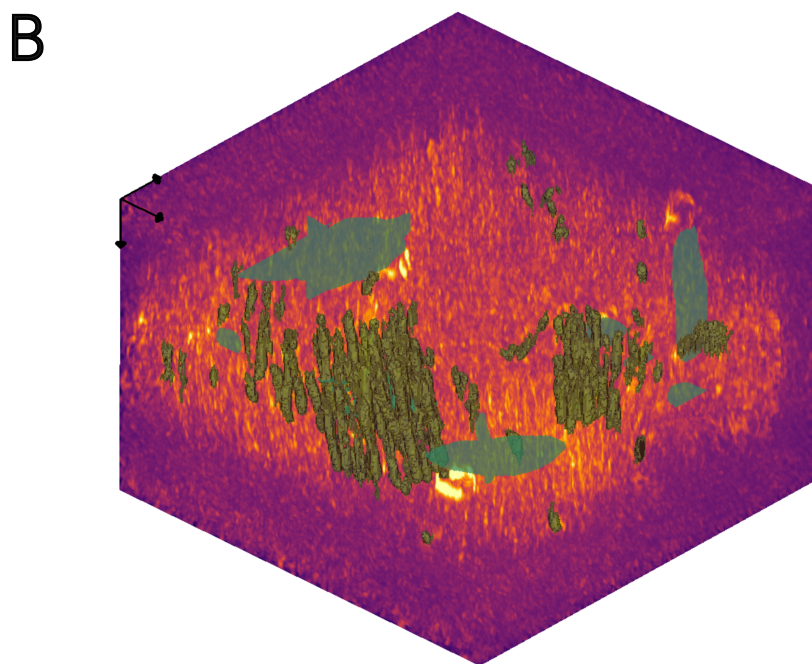
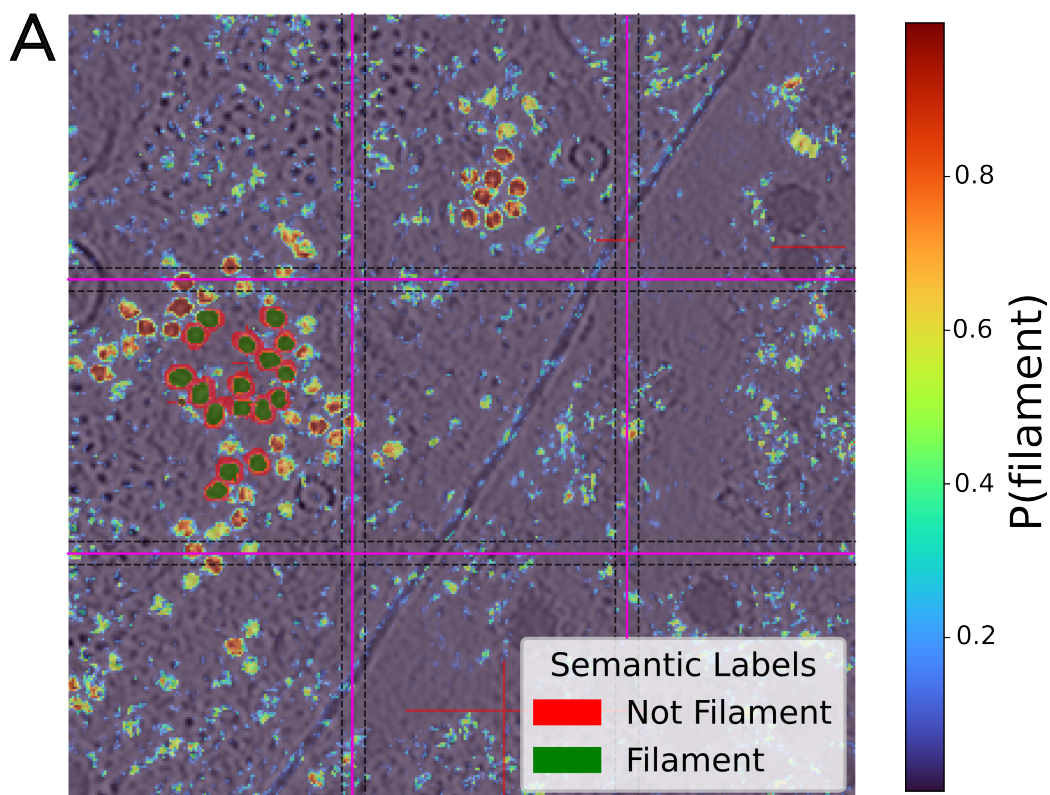


Figure 2: Segmentation results. A - A 2D section of the resulting segmentation of the tomographic data (grey) is overlaid with the class probability map for the intermediary filaments (multi-color heatmap) and part of the hand annotated voxels (green, red). Boundaries of the subsampled tensor are shown as black dotted lines, while the purple solid